The Linearity Performance of a Two-Dimensional, X-ray Proportional Chamber with 0.58 mm Anode Wire Spacing[*]

G. C. Smith and B. Yu

Brookhaven National Laboratory

Upton, New York 11973

October 1994

The Linearity Performance of a Two-Dimensional, X-ray Proportional Chamber with 0.58 mm Anode Wire Spacing*

G.C. Smith and B. Yu

Brookhaven National Laboratory, Upton, New York 11973

Abstract

A method of construction of multiwire chambers has been developed which yields x-ray images with very small non-linearity, in particular that due to anode wire modulation. The technique requires an absorption region in the detector, with the anode and upper cathode wires, which are parallel to one another, in registration with each other. Studies show that the strength of the electric field in the drift region determines the degree of anode wire modulation and, under specific conditions, modulation is halved in period and significantly reduced in amplitude. New interpolating cathodes have been developed to read out position in the other axis, along the anode wire direction. Position resolution in both axes between 100-150 μm FWHM has been achieved. Two-dimensional images of small objects have been taken which show unprecedented linearity.

I. INTRODUCTION

Position sensitive x-ray detectors have an important role in many areas of research. In the specific field of small angle x-ray scattering, the multiwire proportional chamber (MWPC) has proven a very reliable and versatile imaging device, both for static and dynamic studies [1,2]; experiments in astronomy and medicine also utilize this type of detector. Favorable characteristics such as excellent position resolution (100 μm) and linearity (a few per cent differential non-linearity (DFNL)) in the sensing axis along the anode wires, counting rate capability of up to $10^6 s^{-1}$, good detection efficiency and ease of construction in a range of sizes have contributed to the detector's popularity.

One of the proportional chamber's properties that is not so desirable, however, is its position response in the axis across the anode wires; because these wires occupy distinct locations, usually with a pitch of a millimeter or so, avalanches occur at these locations, and a binning, or modulation, of recorded positions occurs. This leads to poorer position resolution and linearity than in the axis along the anode wires.

Little specific work appears to have been carried out to diminish the magnitude of anode wire modulation. It is possible to allow electrons, liberated from the absorption of an x-ray, to diffuse laterally so that they are collected by more than one anode wire; some position interpolation between wires can then be achieved. This was investigated for an astronomy application by Reid et al. [3], and is also a feature of the spherical drift chamber that has been developed for protein crystallography [4]; some deterioration in resolution may occur with this method, however. It is also possible to interpolate position be-

tween wires by using avalanche angular location [5,6], measuring the amplitude of signals on electrodes adjacent to each anode wire; this is generally a rather complex operation and does not lend itself easily to position readout from detectors with many wires.

We have recently investigated, with some considerable success, a technique in which the anode wire pitch is much smaller than normal, and which also employs a special arrangement of cathode wires. This work is part of a continuing effort to improve the performance of MWPCs as x-ray imaging devices, in particular, two-dimensional MWPCs which our group is developing for use in small angle scattering experiments at Brookhaven's National Synchrotron Light Source. The present detector is being developed for an experiment in which the required collecting area is 10 cm by 2 cm.

II. DETECTOR CONSTRUCTION

Fig. 1 shows a schematic diagram of the position encoding electronics for a two-dimensional MWPC with delay line readout on each of the cathodes. A full description of the encoding technique is given in ref. 7 for one-dimensional detectors and ref. 8 for two-dimensional detectors. Delay lines with transit time of 1 μs are used in the present work.

A schematic cross-section of the present detector looking end-on to the anode wires is shown in fig. 2. Throughout this paper, we denote the X-axis as the direction along the anode wires and the Y-axis as the direction across the wires; electron drift is then in the Z-axis. Table 1 is a list of some major design parameters of the detector.

An important feature of this detector is the registration between cathode wires and anode wires. As will be discussed later, this enhances the charge sharing between anode wires, and improves position linearity across the wire direction. Another important feature is the smaller than normal anode wire spacing, which is intended to help improve position resolution in the Y-axis. We know from the performance of previous devices that
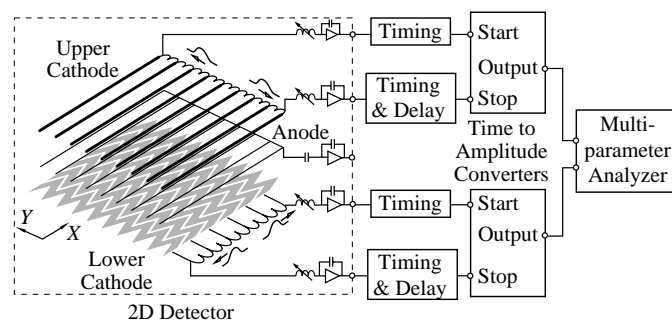

Fig. 1. Schematic diagram of a two-dimensional MWPC using a delay line encoding system.

have been constructed, that an anode wire pitch of greater than 1 mm can result in considerable position modulation in the Y-axis. On the present detector, therefore, an anode wire pitch, $s = 0.58$ mm, was chosen with a cathode wire pitch of the same value. When each cathode wire is connected to each of the 40 nodes on our existing delay line encoding system, this wire pitch conveniently results in a total detector width of just larger than 2 cm.

The distances between the anode wire plane and the two cathode planes, d, are set equally at 0.58 mm, resulting in an s/d ratio of unity. This ratio is a good compromise between the spatial extent of the induced charge distribution on the cathode planes, which increases with d, and the percentage of the total induced charge on the cathode planes, which decreases with s/d [9]. The lower cathode, fabricated from printed circuit board, contains 40 nodes over its 10 cm sensing length; a shorter version of length 5 cm provides enhanced position resolution at lower charge levels over a smaller collecting area. Anode and cathode wires have a pitch accuracy of $\pm 10 \mu$m; registration between anode and cathode wires is accurate to about 30μm.

The entrance window of the detector is made of beryllium, with an area of 10 cm by 2 cm. X-rays with energies in the range of 2 to 12 keV can be detected with good efficiency, using beryllium thicknesses of 25μm to 1 mm, the latter allowing operation at 2 atm. The complete detector is housed in an aluminum enclosure with dimensions of about 25 cm$\times 15$ cm $\times 15$ cm. All experiments reported in this paper were made with 5.4 keV x-rays and an operating gas pressure of 1 atm.

Special care is required in constructing detectors with very small electrode spacings. The critical voltage, that voltage at which anode wires will deflect because of electrostatic repulsion is closely tied to the absolute value of s (and d) [10]; in the present chamber, with anode wires of tension 20g, the critical voltage is approximately twice the operating voltage. It is also important to ensure that the edges of the wire frame are carefully designed in order to avoid surface current between anode and cathode wires. Nevertheless, when proper procedures are followed, the detectors are very stable. MWPCs with anode wire spacings as small as 0.4 mm and 0.2 mm have been previously reported [11].

Table 1: Major parameters of the detector

Anode wire spacing, s	0.58 mm
Anode wire diameter	12μm
Anode, cathode spacing, d	0.58 mm
Cathode wire spacing	0.58 mm
Cathode wire diameter	30μm
Total gas depth	6.35 mm
Area of entrance window	10 cm$\times 2$ cm

III. LINEARITY OF POSITION READOUT

A. Across the Anode Wires

A recent study [12] in which the anode wires and cathode wires were parallel and in registration, but with about twice the wire pitch used here, has revealed the possibility of decreasing the degree of non-linearity by changing the time constant of the
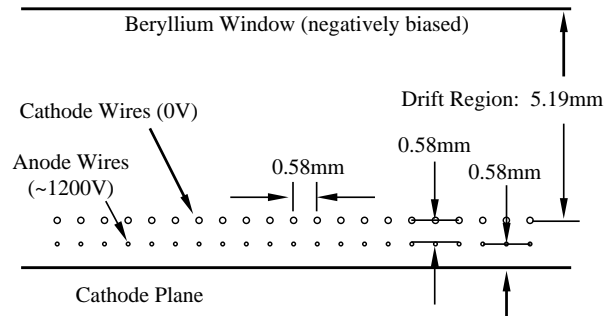

Fig. 2. A cross-section of the new detector

readout electronics, or by changing the electric field in the drift region. In this work, we have studied further the effect of the electric field in the drift region on the anode wire modulation.

A sensitive measure of position linearity can be made by recording detector position response with a beam of x-rays whose intensity is uniform along the axis under test. Uniform irradiation responses (UIRs) were recorded in this manner across the anode wire direction with different bias voltages on the detector window with a gas mixture of Ar/20% CO_2. Three of these UIRs are shown in fig. 3(a) through (c) (the average number of counts in the vertical scale is about 3000 but the ordinate in these and all subsequent UIRs has been normalized to an average of unity). Plots of the electron drift lines from the drift region to the anode wires, and the equipotential contours for the corresponding window voltages are shown in fig. 3(d) through (f); all electrostatic studies were performed with the Garfield simulation program [13]. In the case of zero window bias voltage ($V_w = 0$), the drift field, E_d, is about 280 V/cm, due to leakage of the field in the multiplication region where most of the field is above 10 kV/cm. Because of the very small field ratio ($< 3\%$), electron drift lines originating in the drift region in a cell bounded by two adjacent cathode wires are heavily pinched in the multiplication region into a channel less than 20μm wide, through which the electron cloud from an x-ray converting in the drift region must pass. Diffusion of the electrons during their travel down this extremely narrow channel results in nearly equal quantities of charge sharing between the two corresponding adjacent anode wires, *irrespective* of the Y-axis position of the event in the drift region. The position encoder therefore records these events heavily biased towards the position midway between the two anode wires, as seen in fig. 3(a).

On the other hand, a strong drift field prevents the electron drift lines from forming a very narrow channel, thereby reducing the number of events in which charge sharing between two anode wires occurs. With a window bias voltage of -1400V, $E_d \approx 3$ kV/cm (fig. 3(f)) and the corresponding UIR in fig. 3(c) indicates that indeed there is now a bias of recorded events towards the anode wire position.

When the drift field is optimized, as shown in fig. 3(e), the uniform irradiation response shows that peaks appear both at the anode wire position and at the midpoint between the wires. Under this condition ($V_w = -600$V, $E_d = 1.4$ kV/cm), the anode wire modulation has a period of half the anode wire spacing, and a greatly reduced amplitude.
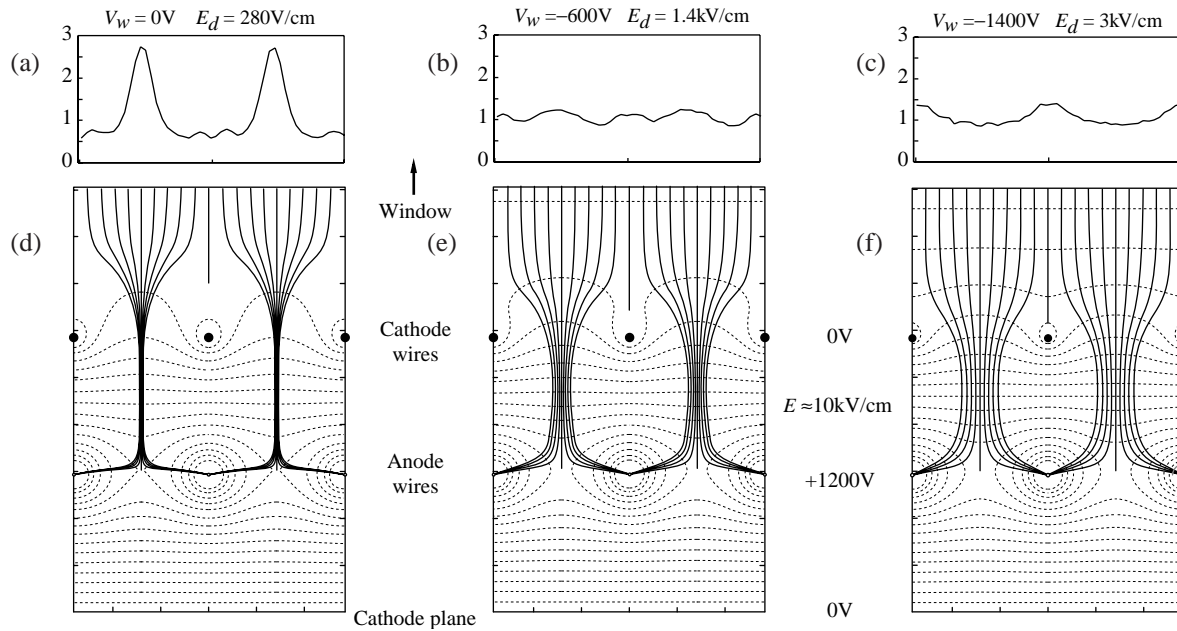
Fig. 3(a),(b),(c) Uniform irradiation response (UIR) spectra across the anode wire direction for three different window bias voltages. The gas mixture used was Ar/20% CO_2. (d),(e),(f) Electron drift lines from the drift region and equipotential contours for the same voltages; tick marks in vertical and horizontal axes are 200 μm apart.

Fig. 4 is a montage of UIRs from eight different window bias voltages in the same gas mixture. The change in the anode wire modulation as a function of the drift field is very dramatic.

It should be noted that the enhanced charge sharing is largely a result of the anode-cathode alignment. In the case where the anode and cathode wires are offset by half a wire pitch, or the number of cathode wires is larger than that of the anode, the benefit of the enhanced charge sharing will not occur.

In order to further understand the non-linearity as a function of drift distance, a finely collimated x-ray beam was directed onto the detector with a 45° angle in the Y-Z plane. Fig. 5(a) illustrates the paths along which electrons generated from the x-ray beam travel. The response of the detector for different drift distances (Z-axis) is now mapped onto its Y-axis. Detector response of the x-ray beam was recorded for several different window bias voltages. Fig. 5(b) shows three of the spectra. The horizontal scale of the spectra is adjusted such that the coordinate system aligns with that of fig. 5(a). (It is worth noting that the UIRs shown in fig. 3 represent the cell by cell averages of the corresponding spectra in fig. 5(b), weighted according to the photon absorption depth.)

The amplitude of the modulation from events that originate in the drift region decreases as the drift field increases, due to the charge sharing process described earlier. In addition, for a given field, the modulation decreases as the drift distance increases, a natural result of greater electron diffusion.

An interesting effect occurs for events absorbed between the two cathode planes. As expected, events are strongly biased towards the anode wires (the three peaks at the right hand side of fig. 5(b)), giving nearly identical responses under different drift field strengths. However, a doublet peak is observed under one section of the x-ray beam. This is due to angular localization of the anode avalanche and the subsequent movement of

the positive ions [14]. Even with a 100 ns shaping time, the separation of the two ion peaks is well resolved because of the very small wire spacing, and a high resolution position encoder in this detector. Further measurements with a xenon based gas, and with different shaping times, show that the separation of the peaks in the doublet increases as ion mobility and shaping time increase.

One of the unexpected results is the fact that even at high drift field, there is no clear sign of drift region events being biased toward the anode wires. This seems to indicate that electron diffusion is large enough that charge sharing dominates for most of the drift region.
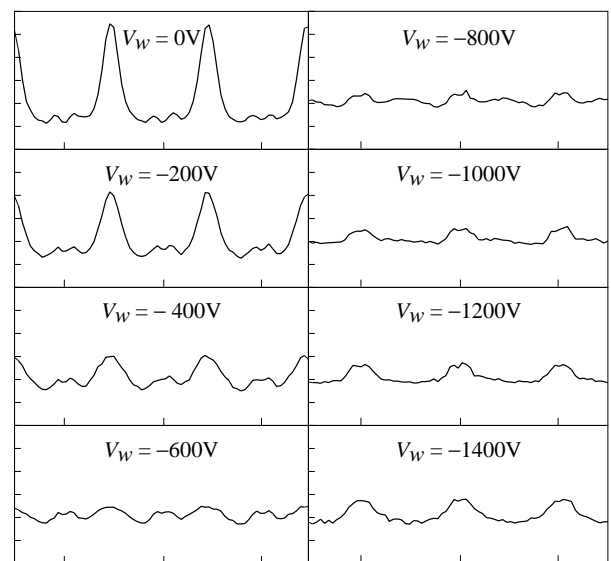

Fig. 4. Eight UIR spectra across the wire direction under different window bias voltages. The gas mixture was Ar/20% CO_2. Tick marks on the abscissa represent anode wire positions.

(a)

X-ray Beam   Beryllium Window

Cathode Wires

Anode Wires

Cathode Plane

(b)

No. of counts

$\cdots\cdots$ $V_W = -300V$ —— $V_W = -600V$ ══ $V_W = -1200V$
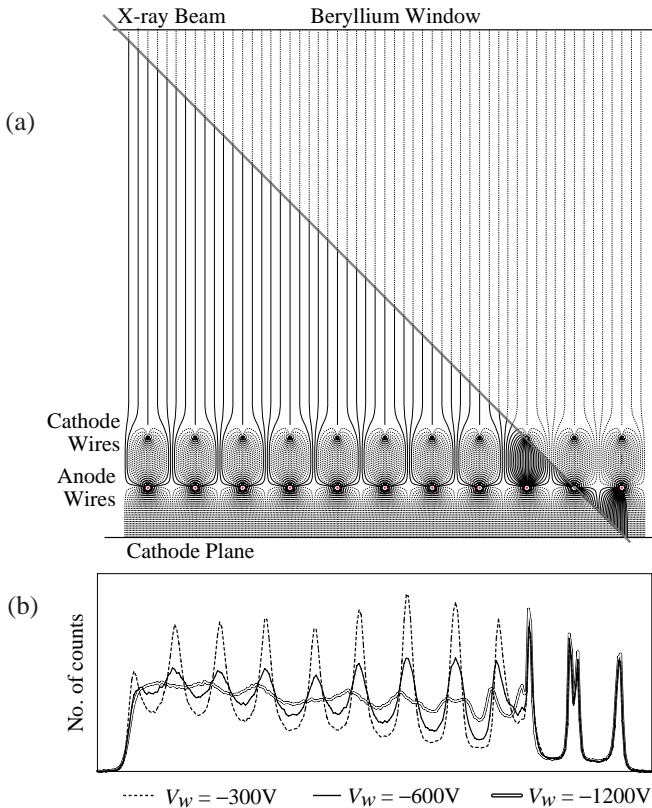
Fig. 5. (a) Plot of electron drift lines for a 5.4 keV x-ray beam incident at a 45° angle. The anode wires are at 1200 V, and the window is biased at -600V. (b) The detector responses for three different window bias voltages; the total count for each spectrum has been normalized. The gas was Ar/20% CO_2.

A comparison of the differential non-linearities in this detector and its predecessor, whose anode wire pitch is 1.1 mm and has no specific alignment between the anode and cathode wires, is shown in fig. 6. The differential non-linearity is determined as: DFNL = $2(I_{max} - I_{min}) / (I_{max} + I_{min})$, where I_{max} and I_{min} are the peak and valley magnitudes in the UIR spectrum. The DFNL in the present detector is about 25% while the previous device is 150%; the improvement in non-linearity is significant. The DFNL in the present detector with Xe/10% CO_2 is even lower, 18%, at least in part due to a larger mean electron drift distance. A further reduction in non-linearity could be achieved by using a deeper drift region, since, as shown in fig. 5, non-linearity reduces as the drift distance increases.
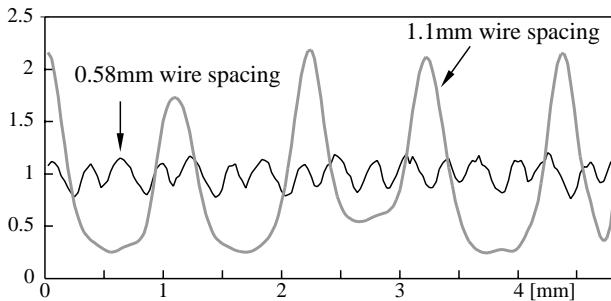

Fig. 6. A comparison of the UIRs across the anode wire direction obtained from this detector and a previous detector [8] with a larger anode wire spacing. The gas was Ar/20% CO_2.

B. Along the Anode Wires

Along the anode wire direction, a printed circuit cathode is used to provide accurate position encoding. A variety of interpolating cathode patterns have been studied by our group prior to this work [15]. However, since *w/d* for the 10 cm cathode is quite large (~4.4), the two intermediate strip (TIS) cathode successfully used in our previous two-dimensional detector would give a very large non-linearity here. A zigzag strip (ZZS) cathode [15,16] and a new single intermediate zigzag strip (SIZS) cathode were developed for the present detector. Fig. 7 is a schematic of these two cathode patterns. The SIZS pattern is a hybrid between a single intermediate strip (SIS) and a ZZS cathode. The slightly greater width of the intermediate zigzag strip improves the linearity of the cathode. Both cathode patterns give excellent position linearity in the X-axis for x-rays (DFNL< 5%). A more complete description of the new cathodes will be given in a later report.

IV. POSITION RESOLUTION

A. Across the Anode Wires

To measure position resolution across the anode wires, a 30 μm wide collimated x-ray beam, incident normally onto the detector, was scanned across the wires in intervals of 1/5 of the anode wire pitch; thus, six position spectra were recorded over a distance equal to *s*. The detector response to 5.4 keV x-rays in argon and xenon is shown in fig. 8.

As was found in the UIR measurements described in the previous section, the tendency for events absorbed between the two cathodes to be biased towards the anode wire positions also has an influence on these position spectra; in a mixture of Ar/20% CO_2 (fig. 8(a)), secondary peaks for some of the x-ray beam positions occur, due to these events. These peaks do not coincide exactly with the anode wire positions, but are displaced slightly towards the main peak because of the combined effect of positive ion movement away from the anode wire and a finite amplifier shaping time. As can be seen in fig. 8, the secondary peaks are separated from their corresponding main peaks by a significant margin.

The fraction of events in the secondary peaks is consistent with absorption depths in the two gases: the 1/*e* depth for 5.4 keV x-rays in Ar/20% CO_2 and Xe/10% CO_2 is approximately 20 mm and 2.7 mm respectively, which, for normal incidence, leads to about 16% and 6% of photons absorbed be-
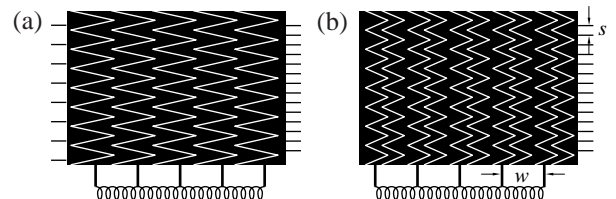

Fig. 7. Schematic drawings of (a) the ZZS, and (b) the SIZS cathode patterns used in this detector. The tick marks on the left side of (a) indicate the anode wire locations in the 5 cm cathode; the tick marks on the right side of (a) and (b) indicate the anode wire locations in the 10 cm cathode. (In the actual device, the wire pitch remains the same.)
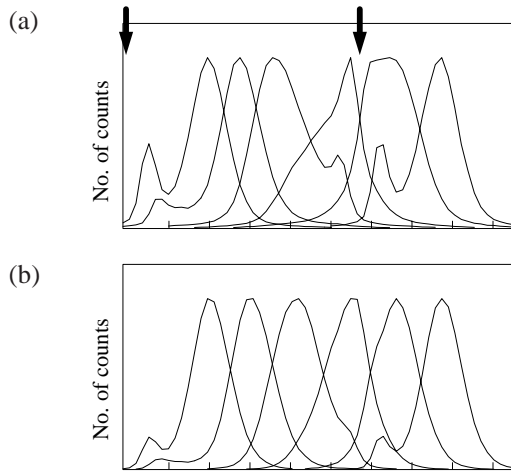
(a)

(b)

Fig. 8. Detector responses (with normalized peak counts) to scans of a collimated x-ray beam across the anode wires at fixed intervals. The detector was filled with the Ar/CO_2 mixture in (a) and the Xe/CO_2 mixture in (b). The distance between tick marks is $100\,\mu m$. The locations of anode wires are indicated by arrows.
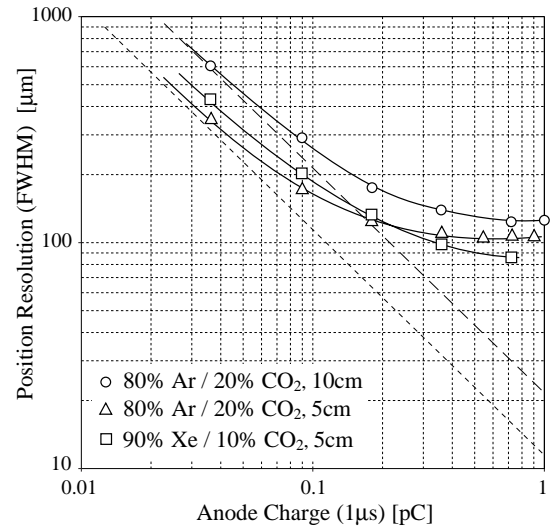

Fig. 9. Position resolution along the anode wire direction as a function of anode charge. The x-ray energy was 5.4 keV. Resolution limited purely by electronic noise is shown by the short and long dashed lines for the 5cm and 10 cm cathodes respectively.

tween the two cathodes. By fitting each of the position spectra to two gaussians, the maximum fraction of events in the secondary peaks is found to be about 18% in the argon gas mixture and 8% for the xenon mixture. These fractions are just a little larger than those from the absorption calculations, possibly because the lower bound of the drift region is slightly above the cathode wire plane (see fig. 5(a)).

Because of the irregular shapes of the x-ray spectra, it is not straightforward to provide an accurate measure of the position resolution in this direction. Nevertheless, some estimates are given to quantify its position resolution. In the argon mixture, the FWHM of the main peaks has a range of $120\text{-}190\,\mu m$, while the rms value of the entire spectrum has a range of $85\text{-}95\,\mu m$. In the xenon mixture, the FWHM of the main peaks ranges from 100 to $140\,\mu m$, while the rms figure of the entire spectrum varies between 60 and $70\,\mu m$.

For many applications of the detector the secondary peaks do not constitute a problem in terms of image linearity. There are, however, steps that can be taken to mitigate their effect:

a) By increasing the drift depth, the relative amplitude of the secondary peaks can be reduced. This has been confirmed by preliminary measurements with an additional gas depth of 6.35 mm between window and wire frame.

b) By use of an electronic discrimination technique, similar in principle to that described in ref. 17, one can take advantage of the fact that the induced cathode signal waveform for events above the anode wire plane has a different pulse height and rise time from events below the anode wire plane. Up to 50% of the events originating between the two cathodes can then be eliminated. In our setup, however, this method uses the direct signal on the planar cathode, and at the moment cannot be used simultaneously with the X-axis delay line encoder.

c) By increasing the shaping time of the cathode readout electronics, the secondary peaks move closer to the main peaks, due to the greater distance moved by the positive ions at

longer shaping times. Further reduction in anode wire spacing should also produce the same effect.

Experimental work on these methods is now in progress.

B. Along the Anode Wires

Position resolution along the anode wire direction has been measured with the same $30\,\mu m$ collimated x-ray beam, with both $Ar/20\%\ CO_2$ and $Xe/10\%\ CO_2$ gas mixtures. The results are shown in fig. 9 as a function of the anode charge as measured in $1\,\mu s$. The best resolution achieved in the xenon mixture is about $85\,\mu m$, and $105\,\mu m$ in the argon mixture, using the cathode with 5 cm length. These measurements are consistent with results in the photoelectron range studies described in ref. 18, indicating that position resolution has reached the gas limit.

Position resolution with a 10 cm zigzag cathode is degraded by about a factor of two at lower charge levels simply because of its length relative to the 5 cm version (see dashed lines in fig. 9); some comment should be made about its best position resolution at higher charge levels. A 10 cm zigzag strip cathode and a 10 cm single intermediate zigzag strip cathode were designed with a zigzag period twice that of the anode wire pitch, in order to avoid the acute angles in the cathode pattern which are more difficult to define accurately with standard printed circuit techniques. This precaution seems to compromise the best position resolution from these two cathodes (about $125\,\mu m$ FWHM) for the following reason. Fig. 10 shows the detector response with the 10 cm SIZS cathode when a collimated x-ray beam is slowly moved along the direction perpendicular to the anode wires; the scan is repeated many times at 1 mm steps along the wire direction. The cathode records wavy lines whose period equals that of the zigzag pattern and whose amplitude varies with the position of the lines. A perfect detector should record a set of straight lines with 1 mm spacing.

This, again, is caused by the movement of the positive ions as a result of angular localization of the anode avalanches.
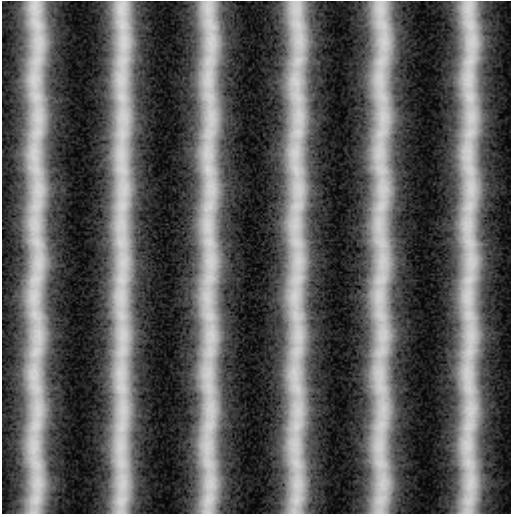
Fig. 10. Detector response to a series of collimated x-ray scans across the wire direction with the 10 cm SIZS cathode. The distance between each scan line is 1 mm. The 10 cm ZZS cathode gives a similar response.

As has been shown earlier (fig. 5 and 8), with the 100 ns shaping time, positive ions have moved a significant distance away from the anode wires. The induced charge distribution on the zigzag cathode is therefore displaced from the wire position by the same distance in the Y-axis, which causes a change in the induced signal ratio between the two adjacent strips directly under the avalanche. This, in turn, results in a displacement of the reconstructed position in the X-axis (fig. 7 shows the zigzag patterns and the location of wires with respect to the pattern). The peak to peak amplitude of the distortion in the worst case is about $\pm25\,\mu m$ for the SIZS cathode and $\pm50\,\mu m$ for the ZZS

cathode. (Similar effects have been reported in a detector with chevron pad cathodes [19].) Since the collimator we used for the position resolution measurement has a rectangular cross-section ($30\,\mu m \times 500\,\mu m$), it is believed that the projection of the wavy pattern along the $500\,\mu m$ length has degraded the measured position resolution.

The above phenomenon is not measurable on the 5 cm zigzag cathode, whose period is equal to the anode wire pitch. Due to the reduction in the zigzag period, the induced charge footprint on the cathode covers relatively more zigzags, resulting in finer charge sampling. An additional improvement is achieved if an event has shared avalanches on two adjacent anode wires: the displacement in the X-axis due to ion movement from one anode wire cancels that from the other. On the basis of this, we expect a considerable reduction in the distortions in the 10 cm cathode by using a SIZS cathode with a zigzag period equal to the anode wire pitch.

V. DISCUSSION

We have presented detailed results from a detector whose anode wire spacing is 0.58 mm, with cathode wires in registration with the anode wires. The non-linearity typically associated with a MWPC across the anode wire direction has been greatly reduced (DFNL~18%) due to diffusion and enhanced charge sharing. To further demonstrate the unprecedented uniform response for both axes in this MWPC, two x-ray transmission images of a 15 mm diameter plastic gear wheel are shown in fig. 11; both images are raw data on a log scale. Fig. 11(b) was taken with an earlier, 10 cm×10 cm detector, in which the anode wire spacing is 1.1 mm and in which there is no specific
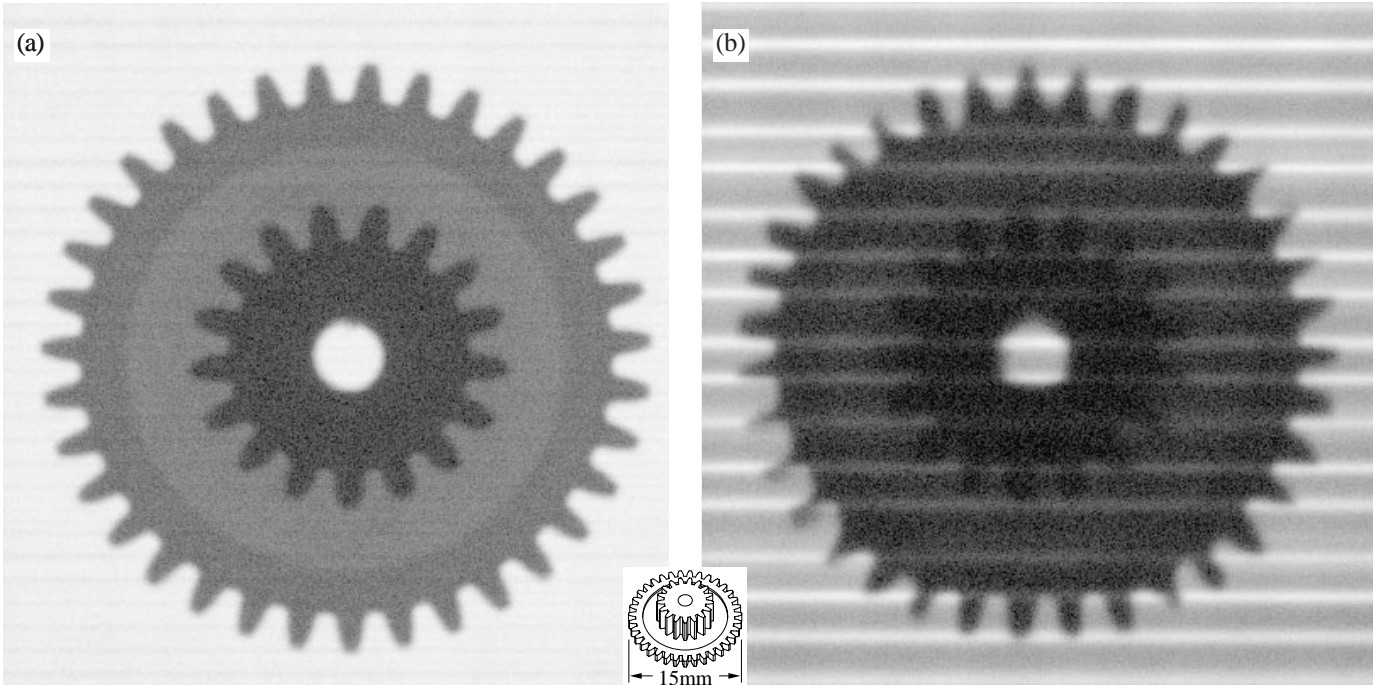

Fig. 11. A comparison of x-ray images of a plastic gear wheel with a diameter of 15 mm (shown life-size in the center), (a) taken from this detector using the Xe/CO_2 gas mixture with a 5 cm zigzag cathode, and (b) from a previous detector [8] with an anode wire spacing of 1.1 mm using the Ar/CO_2 gas mixture. The distance between the gear teeth is about 1 mm. The x-ray energy is 5.4 keV.

alignment of anode and cathode wires. Even though the position linearity in the X-axis is very good, the large non-linearity in the Y-axis, due to the anode wire modulation, results in distortions over the entire image. In particular, there is significant distortion to gear teeth when they are directly in line with an anode wire. In contrast, the image in fig. 11(a), taken by the present detector, shows very little distortion. The definition of all gear teeth is excellent, independent of their positions in relation to the anode wires.

The active area of this new detector is $10\,cm\times2\,cm$. The Y-dimension could be extended by a factor of 3, to $6\,cm$, using the two intermediate strip type of cathode wire readout [8]; this arrangement should not affect the linearity of the system. Further extension in the Y-axis, while maintaining the same wire pitch, becomes difficult due to the limited number of nodes (40) on our existing delay lines.

Purpose built TDCs [20] have already been designed and tested to provide linear response for counting rates up to $10^6\,s^{-1}$ on detectors with the same delay line encoder used here. Replacement of the time to amplitude converters (fig. 1), which have dead times of greater than $10\,\mu s$, with these TDCs, should allow similar counting rate capabilities with this new detector.

The specific anode and cathode wire arrangement that has been described in this paper is equally applicable to MWPCs for detecting charged particles. With a shaping time comparable to the total electron drift time, it should be possible to achieve the same linearity as in these x-ray measurements. In addition, the secondary peaks observed for x-rays should no longer exist because each reconstructed particle track position is the average from many discrete points of ionization along the particle track in the gas volume.

VI. REFERENCES

[1] M.S. Capel, "X12B — A facility for time-resolved x-ray diffraction for biology and macromolecular systems at the NSLS," Synch. Rad. News 6 (1993), 23-27.

[2] R. Lewis et al, "High counting rate gaseous x-ray detectors for synchrotron radiation applications," Rev. Sci. Instrum. 63(1) (1992), 642-647.

[3] P.B. Reid et al, "A drift multiwire proportional counter for cosmic soft x-ray imaging," IEEE Trans. Nucl. Sci. NS-26 (1979), 46-53.

[4] R. Kahn et al, "An area-detector diffractometer for the collection of high resolution and multiwavelength anomalous diffraction data in macromolecular crystallography," Nucl. Instrum. and Meth. A246 (1986), 596-603.

[5] G. Charpak et al, "Progress in high-accuracy proportional chambers," Nucl. Instrum. and Meth. 148 (1978), 471-482.

[6] J. Huth and D. Nygren, "Feasibility tests of a high resolution sampling radial drift chamber," Nucl. Instrum. and Meth. A241 (1985), 375-386.

[7] R.A. Boie et al, "High resolution x-ray gas proportional detector with delay line position sensing for high counting rates," Nucl. Instrum. and Meth. 201 (1982), 93-115.

[8] G.C. Smith et al, "High rate, high resolution, two-dimensional gas proportional detectors for X-ray synchrotron radiation experiments," Nucl. Instrum. and Meth. A323 (1992), 78-85.

[9] E. Gatti et al, "Optimum geometry for strip cathodes or grids in MWPC for avalanche localization along the anode wires," Nucl. Instrum. and Meth. 163 (1979), 83-92.

[10] Particle Data Group, "Review of particle properties," Phys. Rev. D 50 (1994), 1173.

[11] W. Frieze, et al, "A high resolution multiwire proportional chamber system," Nucl. Instrum. and Meth. 136 (1976), 93-97.

[12] E. Mathieson and G.C. Smith, "Performance studies of a multiwire chamber, with 1mm anode wire spacing, to be used for 2-D position-sensitive detection of x-rays," IEEE Trans. Nucl. Sci. NS-37 (1990), 187-191.

[13] R. Veenhof, "Garfield, a drift chamber simulation program," CERN Program Library entry W5050.

[14] J. Fischer, H. Okuno and A.H. Walenta, "Spatial distribution of the avalanche in proportional counters," Nucl. Instrum. and Meth. 151 (1978), 451-460.

[15] E. Mathieson and G.C. Smith, "Reduction in non-linearity in position-sensitive MWPCs," IEEE Trans. Nucl. Sci. NS-36 (1989), 305-310.

[16] T. Miki, R. Itoh and T. Kamae, "Zigzag-shaped pads for cathode readout of a time projection chamber," Nucl. Instrum. and Meth. A236 (1985), 64-68.

[17] C.J. Borkowski and M.K. Kopp, "Electronic discrimination of the effective thickness of proportional counters," IEEE Trans. Nucl. Sci., NS-24 (1977), 287-292.

[18] J. Fischer, G.C. Smith and V. Radeka, "X-ray position resolution in the region of $6\,\mu m$ rms with wire proportional chambers," Nucl. Instrum. and Meth. A252 (1986), 239-245.

[19] B. Yu, "Gas proportional detectors with interpolating cathode pad readout for high track multiplicities," Ph.D Thesis, University of Pittsburgh (1991); BNL Informal Report #47055.

[20] J.A. Harder, "A fast time-to-digital converter for position-sensitive radiation detectors with delay line readouts," Nucl. Instrum. and Meth. A265 (1988), 500-510.